

Optically Controlled Latching and Launching in Soft Actuators

Hongshuang Guo, Arri Priimagi,* and Hao Zeng*

Snapping is an abrupt reaction, in which mechanical instability allows the structure to rapidly switch from one stabilized form to another. Snapping is attained through a sudden release of prestored elastic energy. It is perfected by natural species to enhance their preying, locomotion, and reproduction abilities. Recent developments in responsive materials research has allowed the realization of bioinspired snappers and rapidly moving soft robots triggered by external stimuli. However, it remains a grand challenge to reversibly and accurately control the snapping dynamics in terms of, e.g., onset timing and speed of motion. Here, a facile method to obtain light-fueled snapping-like launching with precise control over the elastic energy released and the onset timing is reported. The elastic energy is prestored in a light-responsive liquid crystal elastomer actuator, and the launching event is dictated by releasing the energy through a photothermally induced crystal-to-liquid transition of a liquid-crystal-line adhesive latch. The method provides manual control over the amount of prestored energy, motion speed upon multiple launching events, and enables demonstrations such as jumping and catapult motions in soft robots and concerted motions of multiple launchers. The results provide a practical solution for controlled fast motions in soft small-scale robotics.

a process in which a bistable structure switches from one form to another through the release of pre-stored elastic energy.^[4,5] Snapping motion enables ultrafast reactions in the time scales of milliseconds or below, yielding extraordinary survival skills for normally slow-moving species, equipping them with, e.g., fast preying, escaping, or seed-spreading capabilities.^[3,6,7]


Inspired by biological actuators, mankind has developed responsive soft material systems that can perform animal-like shape morphing upon different stimuli, such as light,^[8,9] heat,^[10] pH,^[11] magnetism,^[12,13] electricity,^[14] etc. The stimuli-driven active forces produced by these materials resemble the biological muscles driven by chemical fuels. These artificial muscles have led to great interest into the development of bioinspired and biomimetic soft robots,^[15–17] which are often miniature or wireless. Pioneering examples include versatile forms of robotic locomotion, such as externally fueled walking,^[18] jumping,^[19]

1. Introduction

The cruel competitions in biological ecosystem urge fast motions in all forms, across species during their different stages of metamorphosis. However, all natural organisms encounter physical limitations raised by the speed of their muscle actuation.^[1] Millions of years of evolution has allowed many species to overcome this limitation through sophisticated implementation of soft mechanics. For instance, pistol shrimps can rapidly close their claw to shoot out an ultrasound wave bullet to prey,^[2] and larvae of gall midges (*Asphondylia*) can store energy by bending their body and unlatch the energy to jump in order to escape from danger.^[3] Such rapid movements are known as snapping,

swimming,^[20] and flying.^[21] Similar to their natural counterparts, responsive materials encounter limitations in the actuation speed. The speed is affected by the actuation mechanism. For instance, photothermal actuation often occurs in seconds in centimeter-sized samples, due to the requirement of temperature ramp that is often governed by the heat capacity.^[22] Photochemical actuation relies on isomerization of molecular building blocks and concerted motions of these building blocks yield macroscopic shape changes, typically in the time scales of tens of seconds.^[23] Humidity-sensitive actuators rely on the transportation of water across the sample thickness and the motion speed scales with the size of the actuator.^[24,25] To enhance the movement speed of soft actuators, mechanical engineers have utilized snap-through mechanics based on bistable structures.^[26–29] Such mechanics makes use of the prestressed elastomeric layers^[30] or curvature change of stimuli-responsive films,^[31] which often leads to accumulation and instantaneous release of elastic energy. In these systems, the energetics is dictated by the energy barrier of the bistable structure, which does not allow for precise tuning of the snapping power or the timing of the snapping event. An alternative approach is to decouple the energy storage and unlatching processes by using different mechanisms, such as responsive materials for stress generation and magnetic adhesives for stress release to attain launching activity.^[19] However, the mechanical switching process to release the elastic energy usually consumes part of the energy stored and it remains difficult to attain good temporal control. Control over the strength and onset of the snap

H. Guo, A. Priimagi, H. Zeng
Smart Photonic Materials
Faculty of Engineering and Natural Sciences
Tampere University
P. O. Box 541, Tampere FI-33101, Finland
E-mail: arri.priimagi@tuni.fi; hao.zeng@tuni.fi

 The ORCID identification number(s) for the author(s) of this article can be found under <https://doi.org/10.1002/adfm.202108919>.

© 2021 The Authors. Advanced Functional Materials published by Wiley-VCH GmbH. This is an open access article under the terms of the Creative Commons Attribution License, which permits use, distribution and reproduction in any medium, provided the original work is properly cited.

DOI: 10.1002/adfm.202108919

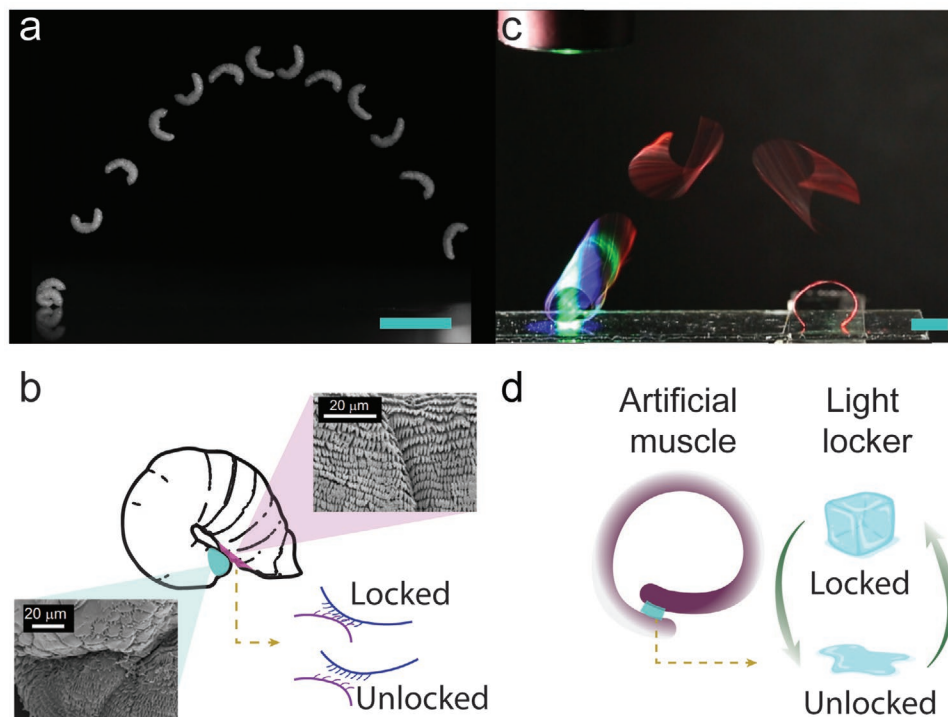


Figure 1. The concept of light-controlled launching. a) Jumping of the larvae of gall midges (*Asphondylia*). b) Schematic drawing of their energy storage and release mechanisms. The insets show the micropatterned surfaces that provide the switching between the high- and low-adhesion states. c) Snapshots of the LCE actuator bouncing in the air in response to the release of elastic energy. d) Light-controlled launcher, in which LCE serves as the artificial muscle and LC adhesive as the mechanical switch. Scale bars in (a) and (c) are 5 mm. (a,b) Reproduced with permission.^[3] Copyright 2019, The Company of Biologists Ltd.

while maintain good efficiency and reversibility are key factors for effective movement (to prey or escape) for soft biological species. Similarly, for responsive-materials-based bioinspired soft robots, an efficient orthogonal control of elastic strength and launching motion is of great significance.

Here, we report a fully optically controlled elastic launching method. We utilize light-responsive liquid crystal elastomer (LCE) actuators as the artificial muscles responsible for elastic energy prestorage upon blue light illumination. The level of accumulated energy is tuned by the irradiation intensity, while the energy release is obtained via a photothermal crystal-to-liquid transition of a liquid-crystalline (LC) adhesive latch sensitive to green light. We demonstrate reversible launching with controlled elastic energy strength, onset, and the speed of actuated motion. Light-controlled catapults and jumping robots are demonstrated as soft robot prototypes. In addition, the reversible crystal-to-liquid transition and the supercooled state of the LC adhesive enables concerted motions of several launchers, and their actuation in series or in parallel. The results offer a facile snapping method for obtaining fast motions in soft actuators, which may bring new advances for optically controlled soft robotics.

2. Results and Discussion

2.1. System Concept

A small-sized, invertebrate soft worm is usually considered to be weak and slowly moving. However, there are examples

in nature, like the one shown in **Figure 1a**, that break this stereotype. The larvae of gall midges (*Asphondylia*) is only few millimeters long, ultrasoft, and fragile, but can perform long-distance jumping through controllable launching action (**Figure 1a**).^[3] To achieve this, the worm intrinsically grows microstructures on two edges of its body (insets of **Figure 1b**). When the worm bends its body into a loop, these micropatterns oppose each other and latch the deformed structure, allowing elastic energy to be stored into its muscles. A slight change of angle between these contacting surfaces significantly decreases the locking force, resulting in a sudden release of elastic energy and instant jumping. The key message from this nature-provided lesson is that effective launching requires an efficient mechanical switch: a mechanism to rapidly change from a high-adhesive (latching) to low-adhesive (unlatching) state. Importantly, such switching itself (through tilting the surfaces) does not consume much of the elastic energy stored, which is particularly important for biological species in view of energy consumption.

Inspired by the jumping larvae, we have designed a light-controlled launcher as shown in **Figure 1c,d**. A splay-aligned LCE actuator strip is used as an artificial muscle for introducing active force upon light illumination. The LCE strip is bent into a loop, and a liquid crystal (LC) glue is used to provide strong adhesive force to latch the geometry, thus allowing the material to store the elastic energy upon illumination. The crystal-to-liquid transition of the LC glue occurs sharply at 55 °C, which enables a sudden drop in adhesion, followed by the release of stored energy and instant jumping

(Figure 1c,d). The materials used in this launching mechanics provide opportunities for precise control over the energy released by tuning the irradiation intensity, efficient latch-unlatch mechanism without consuming its own elastic energy, good reversibility, and orthogonal control of the energy storage and release processes, as will be elaborated in the following sections.

2.2. Photocontrol of the Artificial Muscle and the Mechanical Switch

LCE is a responsive material commonly used in wireless actuators and soft micro robotics.^[32–34] This is due to the fact that LCEs can exhibit large shape transformation in a reversible manner under various types of external stimuli.^[35,36] These stimuli can disrupt the ordering of LC molecules, yielding significant conformational changes in polymer chains and 3D shape-morphing of macroscopic samples.^[37,38] Importantly, such shape changes can be effectively programmed through spatial control over the LC director, and even with uniform material composition the deformations obtained can be multitude, including contraction, bending, twisting, etc.^[39,40] The LCE used in this study is fabricated using chain-extension reaction. The nematic diacrylate monomer and primary amine undergo aza-Michael addition-based step-growth polymerization, resulting in oligomerization of the LC, after which the remaining diacrylate end-groups are cross-linked via photopolymerization, yielding the targeted LCE network.^[41,42] To enable photoactuation, we utilize thermal diffusion of blue-

green-absorbing dye (Dispersed Red 1), which allows for photothermal activation of the LCE deformation.^[43] Further details on material fabrication are given in Figures S1 and S2 of the Supporting Information. The LCE deformation is predetermined by the molecular orientation during the polymerization process. Planar-aligned LCEs contract along the director upon photothermal activation, hence allowing a direct transformation of light energy into mechanical output (Figure 2a,b). Not only can the amount of deformation be controlled by tuning the light intensity, but the large active stress allows heavy mass lifting, up to thousands of times of its own body weight (inset of Figure 2b). All this attests that LCEs are highly attractive artificial muscles, for mimicking the action of biological muscles. To mimic the shape-change of a natural worm, splayed alignment is chosen in the LCE fabrication.^[44] Such alignment results in effective bending deformation raised by the anisotropic thermal expansion between the two surfaces upon photothermal activation (see the infrared camera image in Figure 2c). Thus, through photothermal heating, one can control the temperature of the actuator strip and obtain shape-morphing into different bending angles (Figure 2d). The chemical composition and spectral behavior of the LCE are shown in Figures S1 and S2 of the Supporting Information. Details of sample preparation are given in the Experimental Section.

While the LCE is responsible for light-induced deformation and active force generation, a liquid crystal ester (Synthon Chemicals, ST03866) is used as a phase-controlled adhesive to latch the elasticity. As shown in Figure 2e,f, below 55 °C the adhesive exhibits in a solid form (crystalline state), providing firm connection between a glass sphere and substrate. Above

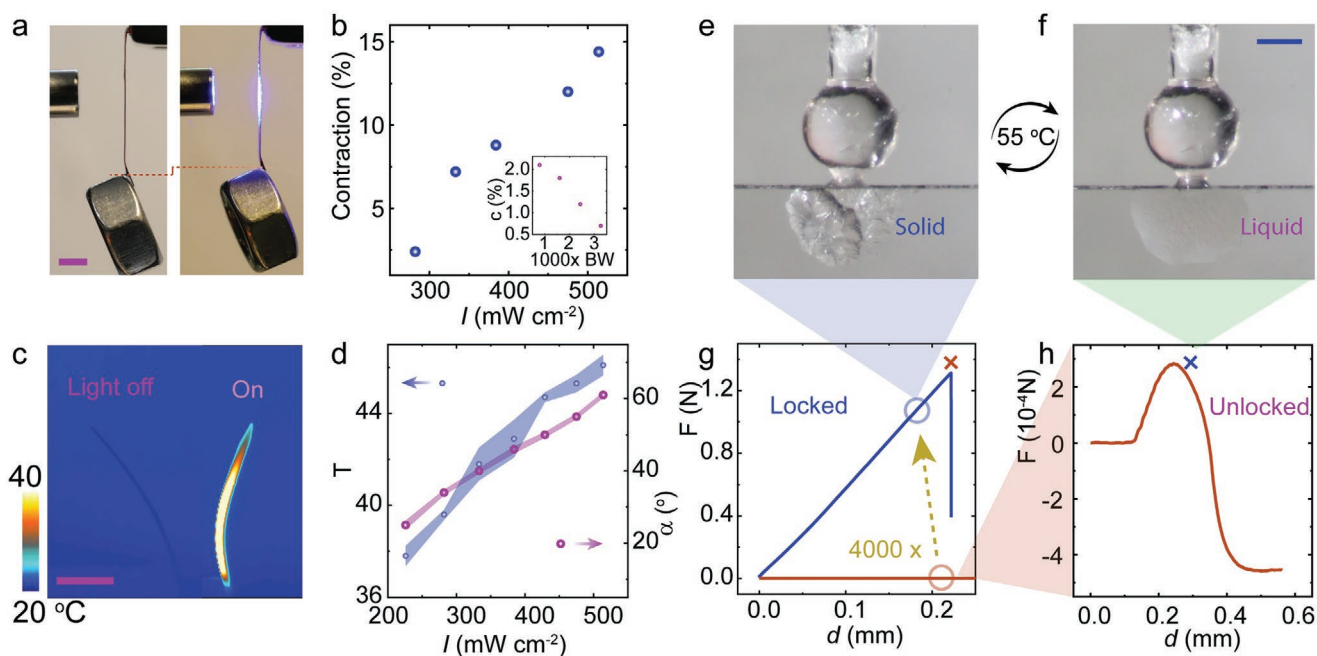


Figure 2. Light controlled muscle and latch. a) A planar LCE lifting an object of 2.1 g, 420 × body weight (BW) under light illumination (460 nm, 340 mW cm⁻²). b) The light-induced contraction of the planar LCE under different light intensities. Inset: LCE contraction, c , under different loadings in the units of body weight (BW) using 510 mW cm⁻² illumination. c) Infrared camera image of a splay-aligned LCE bending under light irradiation (460 nm, 280 mW cm⁻²). Scale bar: 2 mm. d) Light-induced temperature elevation and bending angle of the splay-aligned LCE strip. The error bars indicate standard deviation for $n=3$ measurements. Photographs of the LC adhesive in the e) solid crystalline and f) liquid form. g) Mechanical test of the adhesive force. h) Zoom-in of the adhesive force in the liquid form during the release. Scale bars in (e) and (f): 1 mm.

55 °C the adhesive quickly melts and unlocks the mechanical connection. A mechanical test is conducted to estimate the strength of adhesive force between the two states. The data given in Figure 2g show that the adhesive force in the solid form is up to 1.3 N, and dramatically drops to about 0.3 mN after melting, indicating three orders of magnitude reduction in the adhesive force during the crystal-to-liquid transition. This offers an effective switch for locking/unlocking the launching mechanics. Details of the force measurement are given in the Experimental Section. To introduce optical control over the adhesion, a small amount of dye (Dispersed Red 1, 1 wt%) is doped into the adhesive. This enables photothermal heating of the adhesive with a green laser beam (532 nm) inducing the crystal-to-liquid transition to unlock the launching. Importantly, such phase transition is reversible and occurs sharply at 54 °C (Figure S3, Supporting Information). The melting temperature is slightly lower than for undoped sample, which is expected when dopants are added into LCs.^[45]

2.3. All-Optical Control of the Launching Action

For the launching motion to be practically useful, one should be able to reversibly control the strength and timing, both of which are accomplished with the LCE launcher presented herein, as schematically shown in Figure 3a. Varying the blue light intensity enables different bending force generation (Figure S4, Supporting Information) and different amounts of elastic energy to be stored into the LCE (Figure 3b, see the Experimental Section for further details on the elastic energy estimation). The launching speed (measured by the instant velocity of the tip of LCE strip, Figure S5, Supporting Information; also see the

snapshots in Figure S6, Supporting Information) is dictated by the energy prestored in the LCE, hence depending on the exposed light intensity. The launching velocity is thus light-tunable (Figure 3c). A green laser beam (532 nm, 200 mW, spot size 2 mm) is impinged on the adhesive to induce crystal-to-liquid phase transition through photothermal heating above 54 °C. The excitation wavelength is selected based on the light-absorbing dye used (Dispersed Red 1), and the speed of the temperature increase is determined by the heat capacity of the material. Due to the small volume of the adhesive material, the reaction time, Δt , is well-below a second (Figure 3d). The fast reaction time enables precise control of the onset of launching motion with minimal delay. Note that the storage (obtained using blue light) and release (obtained using green light) of elastic energy are controlled with two different light beams, yielding orthogonal control over the launching dynamics. The energy release is activated at will, rather than triggered passively by crossing the energy barrier of the bistable structure during topological transition.^[26,28] The elasticity of LCE and recrystallization of LC adhesive also enable good reversibility, as exemplified by monitoring the launching speed over multiple events within the same LCE strip under identical illumination conditions (Figure 3e).

2.4. Robotic Demonstrations and Launcher Integration

The all-optical control over the launching dynamics allows realization of LCE microrobots with fast movements. Figure 4a shows a catapult device made of the LCE launcher placed on an oblique (45°) stage. The bending LCE strip is permanently fixed on the bottom of the stage and the top of the strip is fixed

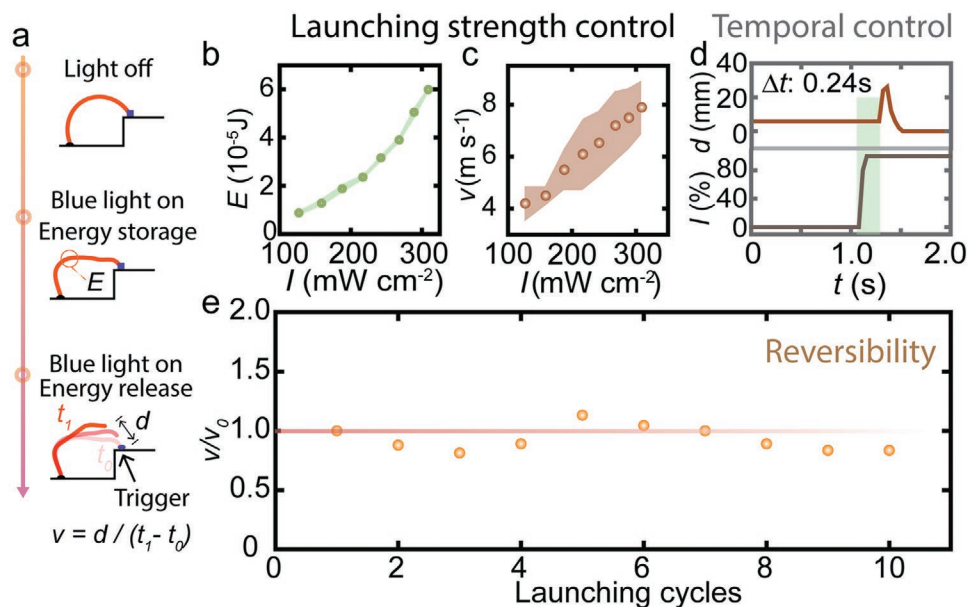


Figure 3. Optically controlled launching. a) Schematic drawing of the light induced launching process of an LCE strip. E , elastic energy; d , tip moving distance; v , launching velocity. b) Light-induced elastic energy stored into the LCE actuator. c) Launching velocity v upon varying the light intensity. d) The time gap (Δt) between incident light excitation and the launching moment. e) Reversibility/reproducibility of the action is estimated by the ratio between v of the strip tip after each launching cycle and the velocity of the first launching event (v_0). Illumination conditions: 460 nm, 160 mW cm⁻². The error bars in (b) and (c) indicate standard deviation for $n = 3$ measurements.

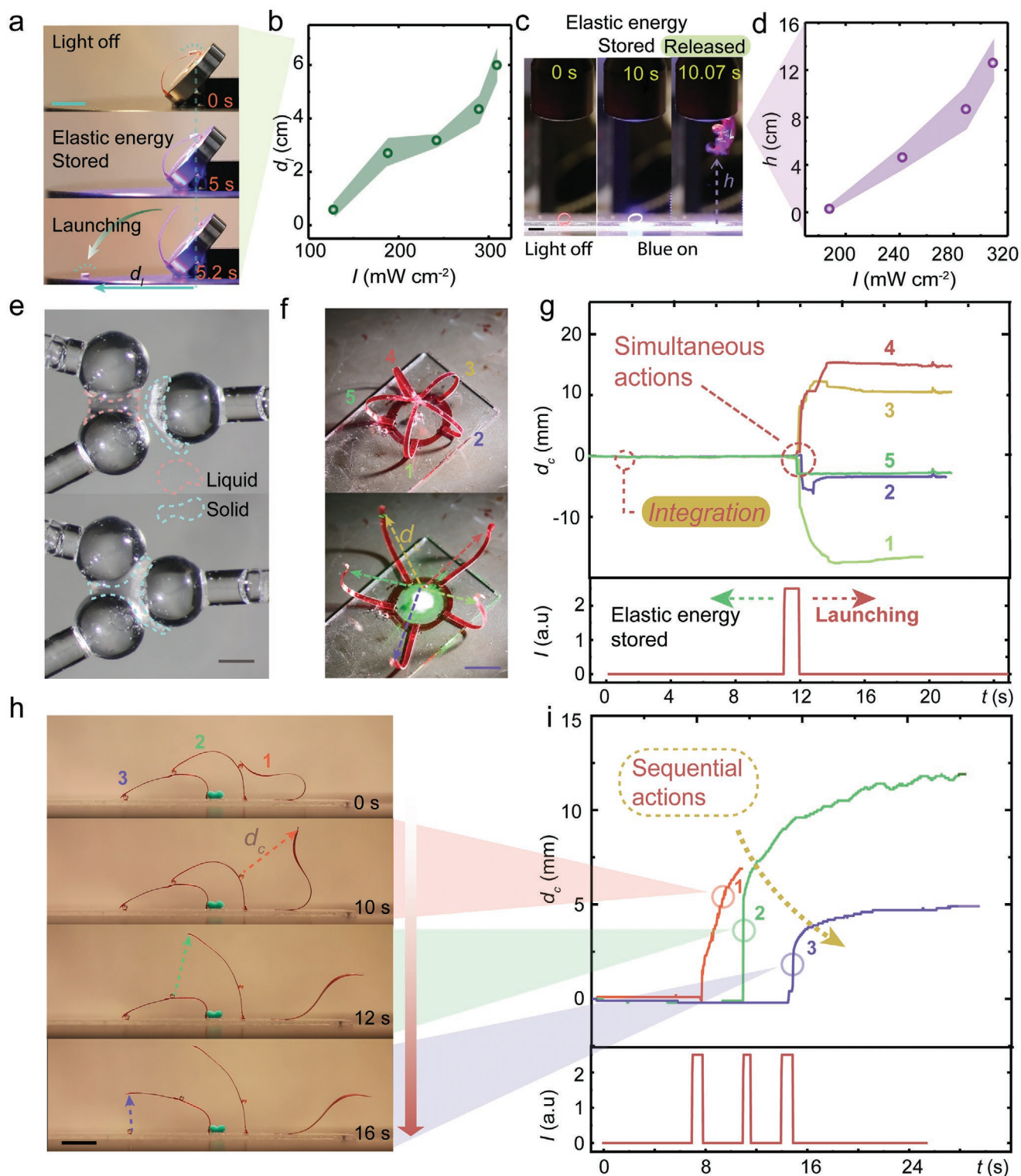


Figure 4. Launching robotics. a) Photographs of light-controlled catapult motion. b) Catapult distance upon varying the excitation intensity (460 nm). c) Photographs of light-controlled jumping. d) Jumping height under different light intensities (460 nm). The error bars in (b), (d) indicate standard deviation for $n=3$ measurements. e) Photographs of the bonding process with the LC adhesive. f) Snapshots of the integrated LCE strips before (top) and after (bottom) launching. g) Displacement of each LCE strip and their association with light excitation. h) Photographs of the sequential light control of three LCE launchers being activated individually. i) Displacement of each sequentially integrated LCE strip and their association with light excitation. In this experiment, the substrate temperature is preset to 50 °C to store the elastic energy without blue-light irradiation, while the energy release is obtained with green laser (532 nm, 200 mW, 2 mm spot size). Scale bars in (a), (c), (f), and (h) are 5 mm, (e) is 1 mm.

with the LC adhesive. A plastic object (20 mg), placed on top of the LCE strip, is used as a mini projectile. The whole strip is illuminated with blue light in order to generate stress and store the elastic energy. Then, a green laser beam is pinpointed to the adhesive to release the energy and propel the projectile (Movie S1, Supporting Information). The catapult distance d_j is recorded as the horizontal spacing between the landing position and the loading point. As shown in Figure 4b, d_j increases from 0.5 to 6 cm by increasing the blue-light illumination intensity from 125 to 300 mW cm⁻². The same principle can be utilized to devise a robot that jumps. As shown in Figure 4c, an LCE strip is bent into a ring geometry, and both ends are fixed together with the adhesive. Upon blue-light illumination (energy storage) and subsequent energy release with green light, jumping action occurs (Movie S2, Supporting Information). In this case, the stored elastic energy is transferred directly into the gravitational potential energy, and the elevating distance of the mass center (jumping height, h) is closely related to the light intensity imposed on the structure (Figure 4d). The jumping height depends on the length of the actuator strip. Upon identical light illumination (290 mW cm⁻²) on samples of the same width (1.5 mm) and thickness (0.1 mm), the maximum jumping distance (9 mm) is obtained with a 13 mm long strip (Figure S7, Supporting Information). A small strip tends to jump higher, transferring larger gravitational energy from its own elasticity during the launching (Figure S7e,f, Supporting Information). In practice, small strips (<12 mm) are difficult to shape into a closed loop geometry through manual gluing. Large strips (>25 mm), in turn, may roll out from the illumination area due to asymmetric deformation (Figure S7d, Supporting Information). For further scale-up of the actuator device, one should consider the mechanical stability upon light excitation and increase the thickness of the actuator strip accordingly, in order to provide sufficient bending stiffness for obtaining large elastic energy.

One practical advantage of using the LC adhesive to latch and unlatch the elasticity is that it can be supercooled, i.e., the material remains in the liquid state for a relatively long time span (>5 min) even when cooled below the phase-transition temperature. Once the supercooled liquid meets its solid counterpart, it quickly crystallizes, yielding sudden fixation of the mechanical structure (Figure 4e; Movie S3, Supporting Information). This provides a facile route to connect multiple objects to integrate multiple launchers. Herein, we demonstrate two forms of integrated soft actuators, one exhibiting simultaneous launching and the other sequential launching. Figure 4f shows the simultaneous launching by integrating five arms of the actuator at the center through the LC adhesive. To fabricate the structure, each LCE strip is permanently fixed on the glass substrate from one end, and with ≈0.5 μL LC adhesive drops on the other end. To integrate these strips, we initially turn one of the adhesive drops into solid by adhering ester powder, while keeping other four in the supercooled liquid state. By connecting all the strips together at the center, the liquid adhesives quickly solidify, yielding tight fixation among the strips. The fabricated structure is placed on a hot plate set at 50 °C to store the elastic energy (for energy storage, heating and blue-light irradiation can be considered analogous). A green laser is then used to trigger the launching event simultaneously in each integrated

LCE strip (Movie S4, Supporting Information). Figure 4g gives the position tracking data for each arm-tip, confirming that all the strips launch simultaneously after a certain delay from the triggering signal (the delay time depending on the intensity of the green laser excitation). By integrating the launchers in another configuration (Figure S8, Supporting Information), the actuation of each strip can be controlled individually. Figure 4h shows three launchers being connected in series, while each strip possesses an adhesive segment to trigger the launching. When the excitation beam arrives at the adhesive sections sequentially, the three launchers are actuated accordingly. See Figure 4h for the details on the tracking of tip position in respect to the excitation signal. The launching process is also visualized in Movie S5 of the Supporting Information.

The light-controlled jumping (Figures 1c and 4c), catapult action, and robotic integration (Figure 4f,h) are all based on the bending deformation mode of the LCE actuator. Generally, LCEs can exhibit diverse forms of shape changes by programming the LC orientation within the elastic network, which opens up versatile opportunities for light-controlled launching activities. Figure S9 of the Supporting Information shows the optically controlled launching based on three basic deformation modes: bending, contraction–expansion, and twisting. By proper placement of the LC adhesive to latch/unlatch the elastic energy, these actuation modes enable very different device performances, such as opposite-bending gripper that can rapidly close (Figure S9a, Supporting Information), vertical launching of a micro-object (Figure S9b, Supporting Information), and switching the direction of an indicator (Figure S9c, Supporting Information).

Due to the reversibility of crystal-to-liquid and liquid-to-crystal transition of the LC adhesive and the structural relaxation upon ceasing the light irradiation, the single-strip actuator can return accurately to its original position after each launching activity, re-establishing the mechanical fixation with the stage via the LC glue. This enables reversible, fully light-controlled launching action (Figure 3e) without any manual interference. Further details on the light-controlled relaunching process in relation to the phase of the LC adhesive are shown in Figure S10 of the Supporting Information. However, the jumping robot and the integrated actuators both require manual fixation after each launching activity. This is due to their largely deformed geometries, prohibiting the structures to return to the original position. To attain full optical control over multiple launching events in these structures, one solution could be to incorporate photochemically actuated liquid crystal network (LCN)^[34] actuator segments into the robotic structure. The photochemically driven LCNs can deform upon UV irradiation (due to photoisomerization of their molecular constituents), maintaining the deformed geometry in the dark for a certain period or returning original state upon visible light exposure. Such LCNs enable fine-tuning the robots' geometry,^[46] thus offering a possible route to reconnect the adhesive via purely optical control without human interference.

3. Conclusions

In conclusion, we report a facile technique for all-optical control over launching dynamics of an LCE soft actuator. A

bending strip based on light-responsive LCE is used as an artificial muscle to prestore elastic energy upon blue light illumination, while crystal-to-liquid phase transition of an LC adhesive is used as a mechanical latch to release the prestored energy and trigger the launching event. This design enables i) control over the launching strength with light, ii) optical control over the onset timing, and iii) reversibility of the launching process through multiple events. The supercooled state of the LC adhesive enables integration of several launchers to form a more complex actuator system. Although this work utilizes LCE-based soft actuators, the same launching mechanism can be extended to other soft systems such as hydrogels, carbon-bilayers, and semi-crystalline rubbers.^[47–49] Hence the concept and robotic demonstrations presented may serve as a useful and general approach to obtain fast and controllable stimuli-triggered motions in small-sized soft robots.

4. Experimental Section

Materials: 1,4-Bis-[4-(6-acryloyloxyhexyloxy)benzoyloxy]-2-methylbenzene (99%, RM82) and 4-Methoxybenzoic acid 4-(6-acryloyloxy-hexyloxy) phenyl ester (ST03866) were purchased from SYNTHON Chemicals GmbH & Co. The ester used as LC adhesive has a monotropic phase behavior, exhibiting crystal-to-isotropic phase transition (melting) at 55 °C upon heating, and nematic LC phase upon cooling below 44 °C. 6-Amino-1-hexanol and dodecylamine from TCI, 2,2-Dimethoxy-2-phenylacetophenone from Sigma-Aldrich, Disperse Red 1 from Merck. All chemicals were used as received.

LCE Film Preparation: A liquid crystal cell was prepared by gluing two coated glass substrates, one with homeotropic alignment layer (JSR OPTMER, 4000 RPM, 1 min, followed by baking at 100 °C for 10 min and 180 °C for 30 min) and the other with rubbed polyvinyl alcohol (PVA, 5% water solution, 4000 RPM, 1 min, baked at 100 °C for 10 min) for uniaxial alignment. 100 µm microspheres (Thermo scientific) were used as spacers to determine the film thickness. The liquid crystal mixture was prepared by mixing 0.16 mol RM82, 0.05 mol 6-Amino-1-hexanol, 0.05 mol dodecylamine, and 2.5 wt% of 2,2-Dimethoxy-2-phenylacetophenone at 85 °C. The mixture was filled into the cell via capillary effect at 85 °C and cooled down to 63 °C (1 °C min⁻¹). The cell was kept in the oven for 24 h at 63 °C to allow azo-Michael addition reaction for oligomerization. Then the sample was irradiated by UV (360 nm, 180 mW cm⁻², 20 min) for polymerization. Finally, the cell was opened by a blade, and strips were cut from the film.

Optical Characterization: Optical images and movies were recorded by using Canon 5D Mark III camera with 100 mm lens. Thermal images were recorded with an infrared camera (FLIR T420BX) with a close-up 2× lens. An LED source (CoolLED pE-4000) and a continuous laser (532 nm, 1W, ROITHNER) were used for light excitation.

Force Measurement: The adhesion at the locking state was measured by connecting a glass pole to a force sensor (ME-Meßsysteme, KD34s) with the liquid crystal adhesive (Synthon Chemicals, ST03866) at its crystal form. The glass pole was lifted by a translation stage, and the pulling force was recorded by the force sensor. The adhesion at the unlocking state was measured by immersing the glass pole tip into the liquid-form adhesive fixed on a sensitive force sensor (F329, Novatech, resolution 4 µN). While the pole was lifted via a translation stage, the capillary adhesive force was recorded by the force sensor.

Elastic Energy Estimation: A splay-aligned LCE strip was hanging vertically with a 0.8 g weight object suspended to its end. The object was lifted by the LCE strip upon 460 nm light illumination. The light-induced elastic energy that can be stored inside LCE is estimated to be the gravitational potential energy increase of the object.

Supporting Information

Supporting Information is available from the Wiley Online Library or from the author.

Acknowledgements

The authors are indebted to Zixuan Deng for assistance with experiments. The authors acknowledge the financial support of the Academy of Finland, provided through an Academy project 324353, postdoctoral grant Nos. 316416 and 326445, and the Flagship Programme on Photonics Research and Innovation, PREIN, No. 320165.

Conflict of Interest

The authors declare no conflict of interest.

Data Availability Statement

The data that support the findings of this study are available from the corresponding author upon reasonable request.

Keywords

jumping, launching, liquid crystal elastomers, photoactuation, snapping

Received: September 3, 2021

Revised: December 1, 2021

Published online:

- [1] R. J. Full, K. Meijer, *Electroactive Polymer (EAP) Actuators as Artificial Muscles: Reality, Potential, and Challenges*, (Ed: Y. Bar-Cohen), SPIE Press, Bellingham WA **2001**, pp. 67–83.
- [2] M. Versluis, B. Schmitz, A. von der Heydt, D. Lohse, *Science* **2000**, 289, 2114.
- [3] G. M. Farley, M. J. Wise, J. S. Harrison, G. P. Sutton, C. Kuo, S. N. Patek, *J. Exp. Biol.* **2019**, 222, jeb201129.
- [4] A. Pandey, D. E. Moulton, D. Vella, D. P. Holmes, *EPL (Europhys. Lett.)* **2014**, 105, 24001.
- [5] R. Sachse, A. Westermeier, M. Mylo, J. Nadasdi, M. Bischoff, T. Speck, S. Poppinga, *Proc. Natl. Acad. Sci. USA* **2020**, 117, 16035.
- [6] Y. Forterre, J. M. Skotheim, J. Dumais, L. Mahadevan, *Nature* **2005**, 433, 421.
- [7] S. Armon, E. Efrati, R. Kupferman, E. Sharon, *Science* **2011**, 333, 1726.
- [8] M. Rogó z, K. Dradrach, C. Xuan, P. Wasylczyk, *Macromol. Rapid Commun.* **2019**, 40, 1900279.
- [9] H. Shahsavan, A. Aghakhani, H. Zeng, Y. Guo, Z. S. Davidson, A. Priimagi, M. Sitti, *Proc. Natl. Acad. Sci. USA* **2020**, 117, 5125.
- [10] Q. L. Zhu, C. Du, Y. Dai, M. Daab, M. Matejdes, J. Breu, W. Hong, Q. Zheng, Z. L. Wu, *Nat. Commun.* **2020**, 11, 5166.
- [11] N. Zhou, X. Cao, X. Du, H. Wang, M. Wang, S. Liu, K. Nguyen, K. Schmidt-Rohr, Q. Xu, G. Liang, B. Xu, *Angew. Chem., Int. Ed.* **2017**, 56, 2623.
- [12] W. Hu, G. Z. Lum, M. Mastrangeli, M. Sitti, *Nature* **2018**, 554, 81.
- [13] H. Gu, Q. Boehler, H. Cui, E. Secchi, G. Savorana, C. De Marco, S. Gervasoni, Q. Peyron, T.-Y. Huang, S. Pane, A. M. Hirt, D. Ahmed, B. J. Nelson, *Nat. Commun.* **2020**, 11, 2637.

- [14] J. Nie, X. Chen, Z. L. Wang, *Adv. Funct. Mater.* **2019**, *29*, 1806351.
- [15] Y. Zhang, Z. Wang, Y. Yang, Q. Chen, X. Qian, Y. Wu, H. Liang, Y. Xu, Y. Wei, Y. Ji, *Sci. Adv.* **2020**, *6*, 8606.
- [16] X. Qian, Y. Zhao, Y. Alsaied, X. Wang, M. Hua, T. Galy, H. Gopalakrishna, Y. Yang, J. Cui, N. Liu, M. Marszewski, L. Pilon, H. Jiang, X. He, *Nat. Nanotechnol.* **2019**, *14*, 1048.
- [17] H. Lu, M. Zhang, Y. Yang, Q. Huang, T. Fukuda, Z. Wang, Y. Shen, *Nat. Commun.* **2018**, *9*, 3944.
- [18] A. H. Gelebart, D. J. Mulder, M. Varga, A. Konya, G. Vantomme, E. W. Meijer, R. L. B. Selinger, D. J. Broer, *Nature* **2017**, *546*, 632.
- [19] C. Ahn, X. Liang, S. Cai, *Adv. Mater. Technol.* **2019**, *4*, 1900185.
- [20] K. E. Peyer, L. Zhang, B. J. Nelson, *Nanoscale* **2013**, *5*, 1259.
- [21] Y. Chen, H. Zhao, J. Mao, P. Chirattananon, E. F. Helbling, N.-s. P. Hyun, D. R. Clarke, R. J. Wood, *Nature* **2019**, *575*, 324.
- [22] T. Wang, D. Torres, F. E. Fernández, C. Wang, N. Sepúlveda, *Sci. Adv.* **2017**, *3*, 1602697.
- [23] M. Lahikainen, H. Zeng, A. Priimagi, *Nat. Commun.* **2018**, *9*, 4148.
- [24] H. Tan, X. Yu, Y. Tu, L. Zhang, *J. Phy. Chem. Lett.* **2019**, *10*, 5542.
- [25] K. W. Kwan, S. J. Li, N. Y. Hau, W.-D. Li, S. P. Feng, A. H. W. Ngan, *Sci. Rob.* **2018**, *3*, 4051.
- [26] Y. Kim, J. van den Berg, A. J. Crosby, *Nat. Mater.* **2021**, *20*, 1695.
- [27] D. Lunni, M. Cianchetti, C. Filippeschi, E. Sinibaldi, B. Mazzolai, *Adv. Mater. Interfaces* **2020**, *7*, 1901310.
- [28] W. Fan, C. Shan, H. Guo, J. Sang, R. Wang, R. Zheng, K. Sui, Z. Nie, *Sci. Adv.* **2019**, *5*, 7174.
- [29] J. Jeon, J.-C. Choi, H. Lee, W. Cho, K. Lee, J. G. Kim, J.-W. Lee, K.-I. Joo, M. Cho, H.-R. Kim, J. J. Wie, *Mater. Today* **2021**, *49*, 97.
- [30] A. Pal, D. Goswami, R. V. Martinez, *Adv. Funct. Mater.* **2020**, *30*, 1906603.
- [31] A. Pal, V. Restrepo, D. Goswami, R. V. Martinez, *Adv. Mater.* **2021**, *33*, 2006939.
- [32] C. P. Ambulo, M. J. Ford, K. Searles, C. Majidi, T. H. Ware, *ACS Appl. Mater. Interfaces* **2021**, *13*, 12805.
- [33] Q. He, Z. Wang, Y. Wang, A. Minori, M. T. Tolley, S. Cai, *Sci. Adv.* **2019**, *5*, 5746.
- [34] M. Pilz da Cunha, M. G. Debije, A. P. H. J. Schenning, *Chem. Soc. Rev.* **2020**, *49*, 6568.
- [35] Y.-Y. Xiao, Z.-C. Jiang, J.-B. Hou, Y. Zhao, *Nat. Commun.* **2021**, *12*, 624.
- [36] Y. Liu, B. Xu, S. Sun, J. Wei, L. Wu, Y. Yu, *Adv. Mater.* **2017**, *29*, 1604792.
- [37] H.-F. Lu, M. Wang, X.-M. Chen, B.-P. Lin, H. Yang, *J. Am. Chem. Soc.* **2019**, *141*, 14364.
- [38] M. López-Valdeolivas, D. Liu, D. J. Broer, C. Sánchez-Somolinos, *Macromol. Rapid Commun.* **2018**, *39*, 1700710.
- [39] T. J. White, D. J. Broer, *Nat. Mater.* **2015**, *14*, 1087.
- [40] Y. Sawa, F. Ye, K. Urayama, T. Takigawa, V. Gimenez-Pinto, R. L. B. Selinger, J. V. Selinger, *Proc. Natl. Acad. Sci. USA* **2011**, *108*, 6364.
- [41] T. H. Ware, M. E. McConney, J. J. Wie, V. P. Tondiglia, T. J. White, *Science* **2015**, *347*, 982.
- [42] H.-H. Yoon, D.-Y. Kim, K.-U. Jeong, S.-k. Ahn, *Macromolecules* **2018**, *51*, 1141.
- [43] O. M. Wani, H. Zeng, A. Priimagi, *Nat. Commun.* **2017**, *8*, 15546.
- [44] G. N. Mol, K. D. Harris, C. W. M. Bastiaansen, D. J. Broer, *Adv. Funct. Mater.* **2005**, *15*, 1155.
- [45] J. Vapaavuori, A. Siiskonen, V. Dichiarante, A. Forni, M. Saccone, T. Pilati, C. Pellerin, A. Shishido, P. Metrangolo, A. Priimagi, *RSC Adv.* **2017**, *7*, 40237.
- [46] M. Yamada, M. Kondo, R. Miyasato, Y. Naka, J.-I. Mamiya, M. Kinoshita, A. Shishido, Y. Yu, C. J. Barrett, T. Ikeda, *J. Mater. Chem.* **2009**, *19*, 60.
- [47] M. Hua, C. Kim, Y. Du, D. Wu, R. Bai, X. He, *Matter* **2021**, *4*, 1029.
- [48] Y. Hu, Q. Ji, M. Huang, L. Chang, C. Zhang, G. Wu, B. Zi, N. Bao, W. Chen, Y. Wu, *Angew. Chem., Int. Ed.* **2021**, *60*, 20511.
- [49] Q. Yang, C. Peng, J. Ren, W. Zhao, W. Zheng, C. Zhang, Y. Hu, X. Zhang, *Adv. Opt. Mater.* **2019**, *7*, 1900784.